ELSEVIER

Bone 37 (2005) 545 – 554

BONE

www.elsevier.com/locate/bone

Bone as an ion exchange organ: Evidence for instantaneous cell-dependent calcium efflux from bone not due to resorption

M. Marenzana[a,b], A.M. Shipley[c], P. Squitiero[b], J.G. Kunkel[b], A. Rubinacci[a,*]

[a]*Bone Metabolic Unit, Sci. Inst. H. San Raffaele, Via Olgettina 60, 20132 Milan, Italy*
[b]*Biology Department, Morrill Science Center, University of Massachusetts Amherst, Amherst, MA 01003, USA*
[c]*Applicable Electronics Inc., Forestdale, MA 02644, USA*

Received 10 September 2004; revised 22 April 2005; accepted 29 April 2005
Available online 19 July 2005

Abstract

The current study tests the hypothesis that basal level and minute-by-minute correction of plasma Ca^{2+} by outward and inward Ca^{2+} fluxes from and into an exchangeable ionic pool in bone is controlled by an active partition system without contributions from the bone remodeling system. Direct real-time measurements of Ca^{2+} fluxes were made using the scanning ion-selective electrode technique (SIET) on living bones maintained ex vivo in physiological conditions. SIET three-dimensional measurements of the local Ca^{2+} concentration gradient (10 μm spatial resolution) were performed on metatarsal bones of weanling mice after drilling a 100-μm hole through the cortex to expose the internal bone extracellular fluid (BECF) to the bathing solution, whose composition mimicked the extracellular fluid (ECF). Influxes of Ca^{2+} towards the center of the cortical hole (15.1 ± 4.2 pmol cm^{-2} s^{-1}) were found in the ECF and were reversed to effluxes (7.4 ± 2.9 pmol cm^{-2} s^{-1}) when calcium was depleted from the ECF, mimicking a plasma demand. The reversal from influx to efflux and vice versa was immediate and fluxes in both directions were steady throughout the experimental time (≥2 h, n = 14). Only the efflux was nullified within 10 min by the addition of 10 mM/L Na-Cyanide (n = 7), demonstrating its cell dependence. The timeframes of the exchanges and the stability of the Ca^{2+} fluxes over time suggest the existence of an exchangeable calcium pool in bone. The calcium efflux dependency on viable cells suggests that an active partition system might play a central role in the short-term error correction of plasma calcium without the contribution of bone remodeling.

Keywords: Plasma calcium homeostasis; Short-term error correction of plasma calcium; Ion-selective vibrating probe; Calcium flux; Osteocyte-bone lining cells synctium

Introduction

The contribution of bone to the regulation of plasma calcium is generally recognized [1–6] but its underlying mechanisms are still a matter of live debate [7–11]. A major object of controversy is the possibility that bone contributes to short-term error correction in calcium homeostasis by calcium movement in and out of bones without activating bone remodeling. The existence of such movement has been hypothesized by taking into account timeframes and rates of calcium exchange at the bone–plasma interface (equivalent to 50 to 100 mM of calcium daily) [12,13]. Even the lower of these figures is 10 times higher than the average daily flux due to bone remodeling, and at least 3 times higher than the component of the daily fluxes, i.e., 1000 mg, in the kidney under PTH control [12]. Rapid calcium exchange is present in a variety of species with values generally consistent with those deduced from plasma radiocalcium disappearance curves, see [9] for review. Based on these reports, it has been suggested that the bone remodeling system, activated by PTH, constitutes a supplemental component of the plasma calcium homeostasis that operates when the short-term error correction mechanisms at the bone–plasma interface are not able to reestablish plasma calcium to the set-point. According to this view, bone

* Corresponding author. Fax: +39 02 2643 3038.
E-mail address: rubinacci.alessandro@hsr.it (A. Rubinacci).

8756-3282/$ - see front matter © 2005 Elsevier Inc. All rights reserved.
doi:10.1016/j.bone.2005.04.036

remodeling should be seen as a long-term error correction mechanism [1,9]. The presence of calcium exchange at the bone–plasma interface, excluding that driven by bone remodeling, implies the presence of an exchangeable calcium pool in bone, which is able to readily release/uptake ionic calcium into/from plasma [5,10], and a "putative bone membrane" controlling both the dynamics of the exchanges and the constitution of the pool [5,14]. While location and constitution of the exchangeable calcium pool as a part of the bone extracellular fluid (BECF) are generally acknowledged, controversy remains about the mechanism underlying its regulation and availability to the plasma.

In an extensive review, Green and Kleeman [5] supported the existence of a functional compartmentalization between the ECF and the BECF based upon evidence provided through indirect experimental approaches. Equilibration of the medium with powdered cortical bone revealed that several ions in the BECF were at a concentration out of equilibrium with the plasma, including three times less calcium [15,16]. The existence of ionic gradients between two compartments of extracellular fluid (systemic versus bone or the reverse), separated by lining cells, implies that these cells possess some kind of transporting-epithelial cell-like properties, having polarized calcium pumps [17,18] as well as Na/K, Na/H, and Cl/HCO_3 exchangers [5,19–21]. This transport is consistent with the formation of gap junctions among adjacent osteoblasts, lining cells and osteocytes, and strongly supports the view that these cells form a functional syncytium [22] that might contribute to the ionic exchanges. This syncytium has been shown to maintain sodium, calcium, potassium, and bicarbonate gradients that are lost in dead tissue [6,14,23–26], thus confirming the pioneering view that BECF cannot be considered simply as a blood ultra-filtrate [27]. However, it is still unclear how it might constitute a bone membrane, and how it acts in regulating calcium fluxes into and out of bone [4,5].

Other models of the short-term error correction mechanisms of plasma calcium have excluded the presence of a functional membrane, supporting the concept of a direct dynamic equilibrium between the bone mineral and the plasma regulated by bone cells: (a) through modulation of the availability of the calcium binding sites present on the hydrated crystals surfaces [7], or (b) by deposition of non-collagenous proteins, having a built-in calcium binding capacity [4,28]. The controversies that have surrounded this matter in the past 50 years mainly depend on the difficulties in determining the ionic composition of the BECF directly, and measuring calcium fluxes in real time at the ECF/BECF interface in living intact bone. The pioneering work of Richard Borgens [25], later proven and extended by this laboratory [6,23,24,29], demonstrates the feasibility of applying vibrating probes to study the translocation of different ionic species into and out of the bone fluid (BECF) from and to the plasma (ECF) by measuring the electrical current associated with such ion exchanges. These studies, using a bone injury model in which a damage through the bone cortex exposes the BECF to the ECF, showed that the steady ionic current into the injury site (point sink) and associated ionic exchanges were cell-dependent [23,25]. The critical components of the current were the ionic species [23–25] for which a concentration gradient between BECF and ECF exists [16,30]. Thus, any gradient between the BECF and the ECF involving a specific ion is actively maintained by the osteocyte-bone lining cell syncytium through a pump–leak system [29].

Since a strong concentration gradient of calcium has been shown to be maintained between the ECF (1.5 mM/L) and the BECF (0.5 mM/L) (Table 1) [1,14,16,30,31], it is conceivable that a pump–leak system might constitute the driving force for such calcium exchange. However, using the voltage-sensitive vibrating probe, the ions carrying the currents must be deduced from the effect of targeted media substitutions. It follows that a specific ion, such as Ca^{2+}, may well be a component of the associated net electrical current measured by the conventional vibrating voltage probe, but it is too small to be detected when medium-targeted substitution was applied [23,32]. However, the three-dimensional scanning ion-selective electrode technique (SIET), applied to the experimental model described above, might be able to characterize the calcium component of the ionic exchanges at the ECF–BECF interface. This method, in fact, is a real-time ultra-sensitive quantitative measurement of the absolute calcium concentration and concentration gradient with a spatial resolution of less than 10 μm^3 [33–35].

The current study tests the hypothesis that basal level and minute-by-minute correction of plasma Ca^{2+} by outward and inward Ca^{2+} fluxes from and into an exchangeable ionic pool in bone are controlled by an active partition system without contributions from the bone remodeling system. The importance of defining this issue, i.e., minute-by-minute correction of the calcium concentration in plasma, is crucial to the determination of the mechanism by which bone is able to control its calcium pool, and respond to a sudden calcium demand from the plasma in the absence of systemic stimuli or the contribution of the remodeling system. The identification of the mechanism by which calcium is moved into and out of bone might lead to the characterization of disturbances in mineral homeostasis not

Table 1
Concentration of the principal ions contained in ECF and BECF reported from the literature [15]

Mineral content	ECF (mM/L)	BECF (mM/L)
Ca	1.5	0.5
Mg	0.7	0.4
K	4	25
Na	140	125
Pi	1.8	1.8
Cl	100	130

yet characterized. Alteration of these short-term mechanisms might be responsible for bone loss by activating long-term error correction mechanisms at the expense of bone mass.

Materials and methods

Incubation media

Living metatarsal bones were immersed in a series of media with physiological concentrations of the ionic species present in plasma, and defined: ECF, Ca^{2+}-free ECF, and HCO_3^--free ECF, depending upon the presence of calcium or bicarbonate (Table 2). Calcium was substituted with mannitol, and bicarbonate with Na-isethionate. Reagents were purchased from Sigma (St. Louis, MO). All experiments on living or dead bones were performed at a controlled temperature, 37°C. The pH was maintained at 7.35 ± 0.1 at 37°C. Measured osmolarity of the ECF (343 mosM) [6] matched the theoretical value (363 mosM) with 5% error. Dead bones were obtained by leaving metatarsals for 24 h in fixative solution made of 4% paraformaldehyde in PBS (pH buffered). After fixation time, bones were re-equilibrated for 3 to 5 days in ECF that was changed daily. For bone metabolic inhibition, a lethal dose of Na-Cyanide (NaCN, Sigma) was dissolved in Ca^{2+}-free ECF in order to obtain a final 10 mM [NaCN] in the bathing medium (70 μl of 1 M NaCN concentrated solution was injected, by a standard 1-mL syringe, in 7 mL bathing medium). This concentration is known to act rapidly with irreversible effects (e.g., tissue death).

Bone samples

As in previous reports [6,23,24], weanling mice (Balb/c ByJ type, Jackson, MA, and Swiss-type locally bred strain), 24 ± 3 days old weighing 16.7 ± 3.6 g, were euthanized with CO_2 in a gas chamber. The back limbs were amputated at the distal tibia epiphysis and immersed in HCO_3^--free ECF to avoid pH changes during manipulations. The metatarsal bones (~7 mm long and 0.5 mm thick) were carefully dissected to avoid damage to the bone surface. All manipulations were carried out on samples immersed in medium with an M3 surgical microscope (Parco). After the bone was freed of soft tissue ensheathments, a transcortical hole of ~100 μm diameter was made with a thin stainless steel dental drill (Mani; Matsutani Seisakusho, Ken, Japan). The animal use protocol was approved by the local (UMass, Amherst, MA) Institutional Animal Care and Use Committee (protocol no. 22-09-19, addendum IACUC license no. 14-R-0036).

Table 2
Composition of the 3 media used in this study

Medium composition	ECF control (mM/L)	Ca^{2+}-free (mM/L)	HCO_3-free (mM/L)
$NaHCO_3$	27	27	0
$NaCl_2$	96	96	96
Na_2HPO4	1.35	1.35	1.35
NaH_2PO_4	0.45	0.45	0.45
KCl	4	4	4
Ca-Lactate	1.5	0	1.5
$MgSO_4$	0.7	0.7	0.7
Na-Isethionate	3.85	3.85	30.85
Glucose	28	28	28
Mannitol	43.75	46.75	43.75
HEPES	10	10	10

Calculated osmolarity for all media was 363. Measured osmolarity for all media was 343.

Scanning ion-selective electrode technique (SIET)—basic principles

SIET has been used extensively in the past 15 years [36–39] and key reviews are available [32,33,40]. SIET measures the free-ion concentration gradient of a specific ion (calcium here) by means of an ion-selective microelectrode (ISM) "vibrated" (repeatedly moved between measurement points using stepper motors) at a selected distance (5 to 50 μm excursion) in the bulk media at programmed repetition rates slower than 1 Hz (typically 0.3 to 0.5 Hz range). A move-wait-measure scheme is employed. Global positioning of the ISM, stepping excursion, and sampling times for differential measurements are software programmable. The ISM records a voltage at each measurement point representing the local concentration of the ion being measured. All voltages are referred to a grounded Ag/AgCl electrode via a salt bridge (3 M KCl with 3% agar inside 1.5 mm diameter polyethylene tube) in a fixed place in the bath a few millimeters away from the stepping ISM. Baseline or reference is established at locations in the bath millimeters away from the specimen (no gradient detectable). All measurements at the specimen are referred to reference readings taken periodically during the experiment. Each gradient data point is given by subtraction of the ion concentration values measured at each position. The flux is derived from Fick's law of diffusion:

$$J = -D(\mathrm{d}c/\mathrm{d}x) \quad (1)$$

where J is the ion flux in x direction, $\mathrm{d}c/\mathrm{d}x$ is its concentration gradient and D is its diffusion constant. The direction of the flux is derived from Fick's law of diffusion that relates the concentration gradient to the diffusion coefficient. The sign of the gradient, in turn, depends on the convention by which it is measured, i.e., the direction of vibration. Accordingly, a positive chemical gradient ($\mathrm{d}c/\mathrm{d}x$) is calculated when the origin point is at a lower concentration compared to the sample point, thus the calculated flux (J), directed from sample point to the origin, has a negative sign. The origin point was the measurement point away from the bone surface and the

sample point was the measurement point near the bone surface. For interpretive and display reasons, a calcium efflux from the bone is negative whereas an influx into the bone is positive.

SIET—setup and calcium measurement method

The reference electrode was an Ag/AgCl half cell (#MEH3S, World Precision Instruments, Inc., FL, USA), connected to the solution by a PVC capillary tube filled with 3 M KCl and 0.5% agar, and the ISM was a glass capillary pulled in two stages (tip 3–5 μm) on a Flaming Brown Model P-97 electrode puller (Sutter Instruments, Novato, CA) that was backfilled with 100 mM $CaCl_2$ electrolyte and frontloaded with a 30- to 40-μm-long column of liquid ion exchanger (LIX) (Fluka Chemie AG Ca^{2+} ionophore 1, cocktail A, Buchs, Switzerland).

The layout of the SIET setup showing its principal components is sketched in Fig. 1. The probe voltage, proportional to Ca^{2+} concentration, was amplified by a direct-coupled (DC) amplifier (Applicable Electronics, Inc. Forestdale, MA 02644, USA) similar to the setup originally reported by Jaffe and Levy [36]. The ISM probe was mounted to a three-dimensional micromanipulator (NEWPORT Corp., Fountain Valley, CA) 300 series translation stages, 50 mm travel, driven by stepper motors. This allows scanning the microelectrode over an area of 50 × 50 mm while also "vibrating" (repeatedly stepping from an origin point to other test points). The motors were controlled with a CMC-4 four-axis micro-step motion controller (Applicable Electronics, Inc.). This combination of hardware and software provides spatial accuracy of less than 0.5 μm. The ISM was programmed to step using automated scanning electrode technique software (ASET, v.105 software, Science Wares, Falmouth, MA, USA).

The ISM was stepped three-dimensionally from an origin point along the x, y, and z axes. Step excursions ranging 10–30 μm were set for all axes (x, y, z) based on the experiment-to-experiment signal-to-noise ratio. Improvement in precision of a measurement at a particular location was increased by repeating the basic self-referenced measurement.

Motion control and data acquisition were controlled by an IBM compatible personal computer with a CIO-DAS1602/16 analog–digital board (Measurement Computing Corporation, Middleboro, MA). The ASET software calculates the Ca^{2+} concentration gradient using the voltage difference (in μV) between paired points in space along each direction of stepping (x, y, z axes). Microvolt values (μV) were converted to tip flux units (pmol cm^{-2} s^{-1}) using Ca^{2+} calibration data from each probe and the Nernst equation. Calculations of [Ca^{2+}] were recorded at each end of the stepping excursion (10 or 30 μm) between the extremes of the excursion to determine the local calcium gradient. Computation of fluxes from artificial sources was performed as previously described [37,41]. Briefly, the flux emanating from a point source and measured at the surface of a radially surrounding sphere was assumed to be uniform on the sphere and Fick's law of diffusion was used to compute flux.

A two-point calibration of the ISM was done by recording the static mV reading (averaged over 5 s) from two standard calibration solutions (1 and 10 mM [Ca^{2+}]). ASET automatically calculates the Nernst slope from these two values. ISMs with non-Nernstian slopes were discarded. The dynamic efficiency of the particular ISMs used in this work, was 90%, whose value depends on many factors

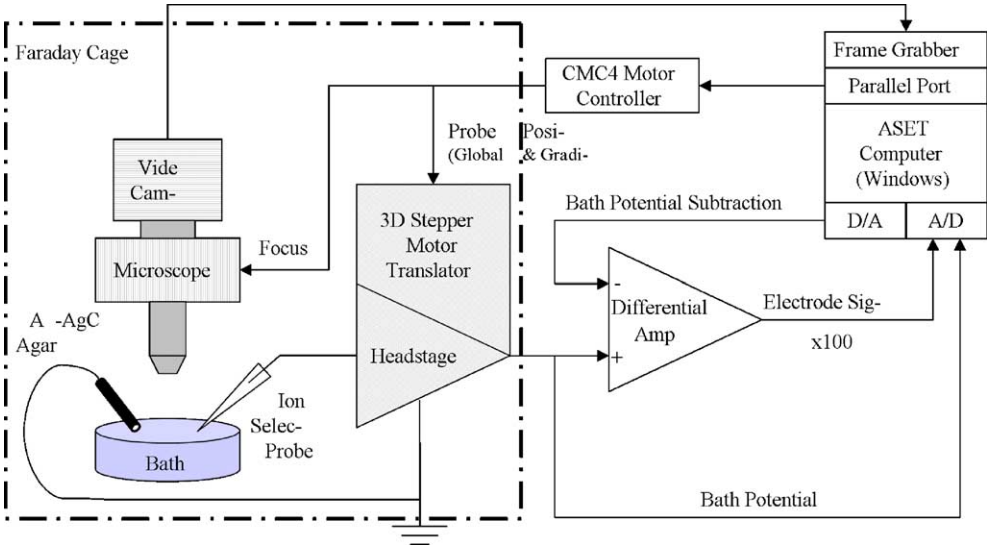

Fig. 1. Block diagram of the SIET system (only one channel shown). Note that the system has an auto-zero feature that provides cancellation of the ISM Nernst potential (bath potential) to maximize the A/D board dynamic range (±10 VDC). This allows for very high gain in a DC-coupled system (up to 1000×). The dashed box represents a Faraday cage that enclosed the experimental stage. The inside of the cage was covered with an insulating layer which helped the temperature control system to maintain the entire cage at the steady temperature of 37°C. Experiments were performed with the cage doors closed. The CCD video camera on the microscope provided a visual display of the probe and specimen under study.

including tip size, signal amplification, and programmed sampling times [41].

Typically, a new ISM was made and calibrated each day. The background bulk calcium concentration was first measured by placing the ISM far from the bone sample (10 mm). Using the 3D motion system, the probe was moved to the recording site, around 50 μm above the cortical hole, to detect calcium fluxes. Static mV and μV difference values stabilized around 5 to 10 min after medium exchanges. The coefficient of variation, defined as SE/average when the location was kept constant (with probe moving back and forth between a given location and a reference point) was less than 5%.

Experimental setup and data acquisition

The experimental setup is similar to the one previously described for the voltage vibrating probe [6,23,24,29] except for the substitution of the voltage probe with an ISM and the enclosure of the whole setup inside a temperature-controlled Faraday cage (Applicable Electronics, Inc.). The cage is necessary for shielding the setup from electrical noise due to the very high resistance (GΩ range) of these kinds of ISMs. Briefly, all equipment (chamber, probe electrode, and microscope) was placed on a vibration isolation table (TMC #53-633, Technical Manufacturing Corporation, Peabody, MA). The metatarsal was held (by drops of cyanoacrilate glue) at the extremities on pieces of a nylon washer cut in half fixed at the bottom of a standard 10-cm plastic Petri dish. The dish was filled with the appropriate pre-warmed (37°C) medium and positioned on the viewing stage. Then, the ISM was immersed in the medium; then, the medium surface was covered with a thin layer of light, clear, mineral oil (Mineral Oil, Squib). Contact between the oil layer and the ISM tip was avoided because the oil destroys the ISM probe. The oil layer greatly reduces temperature-driven convection flow in the medium that causes instability in the calcium gradient and helps maintain pH by minimizing air exchanges at the surface of the solution. The oil layer also allows microscopic viewing of the specimen without any obstructions.

The environment inside the Faraday cage was maintained by a temperature controller (Omega, iSeries) measuring the air temperature close to the Petri dish that controlled two quartz heaters bolted to the vibration isolation table top to supply heat. One heater element was constantly on while the other was controlled to maintain temperature (37°C) inside the Faraday cage environment. Two slowly moving muffin fans were used for air circulation inside the Faraday cage to maintain a stable air temperature at the experimental bath. A video CCD camera (Sony DC-393) was placed on an Optem Zoom 70 video zoom scope (magnification range: 5–45×, Thales-Optem, Fairport, NY, USA) and connected to a SONY PVM14N5U monitor and then to an image acquisition card, ComputerEyes/1024, installed in the PC. Light was provided through fiber-optic cables (Olympus) connected to a light source (Fiberoptics Technology). In this way, it was possible to run the experiment within the closed Faraday cage and visualize the motion of the probe on the video monitor outside. The cage was opened briefly for medium changes (2 to 5 min) to allow access to the Petri dish containing metatarsals. A thin, clear vinyl curtain with a slit in the middle covered the access to the Faraday cage to minimize heat loss when the doors were open. After medium changes, recording was restarted after approximately 5 min to reestablish temperature in the cage and the new solution.

Experimental protocol

After testing for the spatial distribution of the calcium fluxes over the metatarsal injury site, the ISM was located at the point of maximal flux (Fig. 2A). The flux magnitude was first recorded in the ECF and then in Ca^{2+}-free ECF. The ISM was positioned at the same location before and after media swaps. Medium substitution was done by repetitive siphoning away (via a vacuum line) and adding in medium (using a standard 5-mL disposable syringe). This was done at least three times to ensure a thorough medium exchange. All experiments were performed at 37°C, pH 7.35 ± 0.1 at 37°C. Total elapsed time for the experiments was about 2 h. The same medium was left in the dish no longer than 30 min. This is the timeframe in which pH is known to be stable in this setup from previous experiments [6,23,24].

For split metatarsals, the maximal flux was localized normal to the bone cortexes at either side of the medullary cavity. Then, a cross-section scan over the entire split bone, starting from one cortex to the other, was repeated 3 times via the ASET software.

Statistics

Data are expressed as means ± SD. Data groups were compared by a two-tailed Student's t test for unpaired observations. Differences were considered significant for $P < 0.05$.

Results

In the control condition with the bone bathed in a medium having the same ionic composition as the plasma, a net influx of calcium entering the site of damage was recorded in all metatarsal bones tested ($n = 32$). The maximal calcium influx was normal to the bone surface at the site of damage, whereas moving away from the site of damage, the calcium influx decreased. The influx was determined from the measured gradients by the calculations described above (see Materials and methods section). The influx was steady from its first recording throughout the

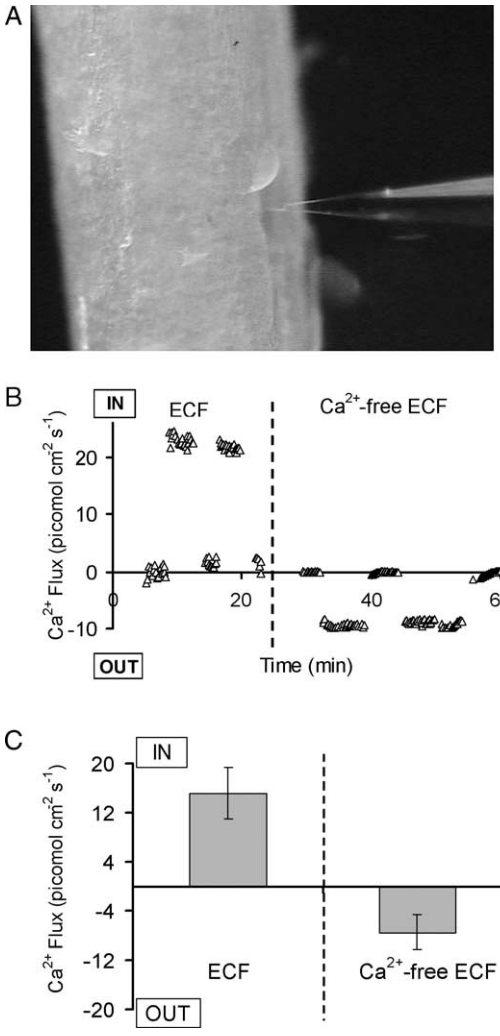

Fig. 2. (A) Microscopic view of the metatarsal bone mounted in the experimental stage with the ion-selective microelectrode at the center of the hole drilled through the cortex. (B) A typical measurement plot shows an initial steady influx at the injury site on the bone immersed in ECF (INward) and its prompt reversal (OUTward) as soon as the ECF was substituted with Ca^{2+}-free ECF (at the dash line). The readings were not continuous because when the media were changed, the probe was moved far away (5 mm) from the bone surface for a reference stability check as well as being in a safe place while changing media. (C) Histogram reporting mean values of influx in ECF and efflux in Ca^{2+}-free ECF expressed in pmol cm^{-2} s^{-1}. Bars represent SD (n = 14).

experimental time (~2 h). At steady state, the calcium influx ranged from 22.4 to 7.9 pmol cm^{-2} s^{-1}, averaging 15.1 ± 4.2 pmol cm^{-2} s^{-1} (n = 14, Figs. 2B,C). In search of the source of the calcium gradient, the probe was scanned over an entire bone transversally split. The calcium efflux, recorded on the inner halves of living split metatarsals in Ca^{2+}-free ECF (Fig. 3), was comparable to that recorded at the center of the hole in the intact bone and reached its maximum over the exposed cortexes, indicating that these were the areas of maximal ion leak.

By removing calcium from the external medium (ECF), the direction of the calcium gradient was immediately

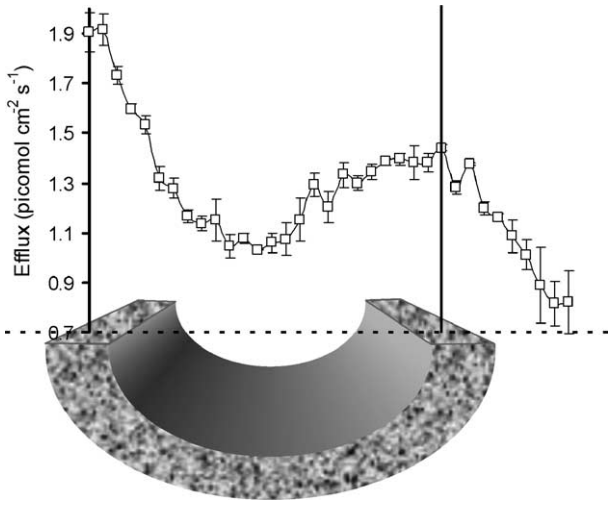

Fig. 3. Sketch depicting the distribution of calcium fluxes recorded on split metatarsals, as obtained by transverse scanning (along the dashed line) with the ISM. Bone is geometrically represented as a cylinder split with an angle of ~35°, as the metatarsals. Note how the efflux (here with inverted sign, for representation purposes) reaches its two peaks in the proximity of the two open cortexes.

reversed and a calcium efflux was recorded ranging from 3.94 to 13.6 pmol cm^{-2} s^{-1} and averaging 7.4 ± 2.9 pmol cm^{-2} s^{-1} (n = 14, Figs. 2B,C). The efflux was steady from its first recording throughout the experimental time of about 2 h. No substantial decrease was observed for up to 4 h.

The efflux in Ca^{2+}-free medium was rapidly shut down by adding 10 mM/L NaCN (Fig. 4). The typical dynamic of the calcium gradient changed with metabolic inhibition showing a biphasic pattern with a transient enhancement of the efflux followed by a subsequent decay to background level within 10 min.

By reconstituting the calcium concentration of normal ECF after cell metabolic inhibition by NaCN addition in Ca^{2+}-free ECF, the calcium influx was recovered, unaffected by alterations in the energy status of the bone cells. In addition, the calcium influx was still present in dead bones re-equilibrated in ECF for 3 to 5 days (16.65 ± 0.37 pmol cm^{-2} s^{-1}, n = 3).

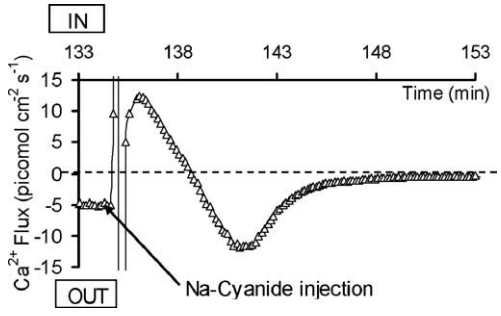

Fig. 4. Representative graph of the efflux dynamics after metabolic inhibition of bone cells by addition of Na-Cyanide to a final concentration of 10 mM/L. The efflux transiently increased after an inconsistent reversal (not shown by all samples), and fell rapidly to background level within 10 min.

The time (T_{eq}) required to reach Ca^{2+} equilibrium between BECF and Ca^{2+}-free ECF was estimated applying the geometric model[1] and using the following assumptions:

a) the volumetric cortical porosity is 5% [42]; hence, BECF volume equals 5% of the total cortical volume and the exchangeable Ca^{2+} pool amounts to 22 pmol for a BECF [Ca^{2+}] of 0.5 mmol/L,
b) only simple diffusion through the chemical gradient (i.e., at a rate of 4 pmol cm^{-2} s^{-1}) is the driving force.

T_{eq} ranged from minutes to hours depending upon the bone surface area that was considered as the source of Ca^{2+} diffusion, such that:

1) T_{eq} = 95 h for diffusion through the point sink (open cortex at the damage site: 0.03 mm^2); or
2) T_{eq} = 2.5 min for diffusion through all the intact surfaces at the quiescent bone surfaces (Q-BS).

Discussion

The results of the current study have shown that: (i) a steady calcium influx occurs in living bone that is immersed in an ionic medium that mimics normal plasma, and is immediately reversed to an efflux when calcium is removed from the medium; (ii) while the calcium influx into the bone is a passive, concentration-dependent process, the efflux from the bone was dependent upon the energy status of the bone cells.

The present study introduces a novelty in the debate on plasma calcium control by bone by recording the first real-time measurement of calcium fluxes at the ECF–BECF interface and so demonstrating that cells are the driving force for the calcium efflux from bone to blood, whose controlling factors, as stated in Talmage's editorial [11], have never been identified.

The experimental model [6,23–25], on which the current work is based, has previously demonstrated the ability of bone to operate as an ion exchange organ. As discussed, the damage tends to short-circuit the potential difference at the damage site (point sink of the ionic current associated with the ionic exchanges). As a consequence, ions are free to move down their electrical/chemical gradients at the damaged site (leak) and the pumps, devoted to the maintenance of the gradients, are activated. The activation of the pump–leak system tends to reestablish the basal ionic gradients. The measurement of this activity at the damage site gives reliable information of the exchanges occurring at the ECF–BECF interface to which the bone as a whole organ contributes.

By applying the SIET, this study achieved three major advances as described in the following subsections.

Quantitative and qualitative estimation of calcium exchange

Direct comparison to previously reported in vitro calcium fluxes can be made with the hypothesis that the local flux measured at the damage site is uniformly distributed on all the available exchange surfaces [i.e., the quiescent bone surfaces $(Q\text{-}BS)^i$]. Under this assumption, an estimate of the average Ca^{2+} net mass transfer rate for the entire metatarsal bone can be computed (1.02 to 2.55 nmol/h $bone^{-1}$). These figures are consistent with the rates measured by Bushinsky and coworkers [3] (2.13 nmol/h $bone^{-1}$) in whole neonatal rat calvariae placed in similar experimental conditions. These in vitro fluxes appear higher (~one order of magnitude) than that expected on the basis of in vivo radiocalcium studies [43] but: (a) the damage (point sink of the Ca^{2+} flux) has the effect to expose BECF to ECF, thus maximally activating the pump–leak system devoted to the maintenance of the electrochemical gradient; (b) cells in a growing animal are perhaps on a heightened metabolic state with respect to calcium metabolism since they are competing to create the bone.

The prompt establishment of the calcium fluxes into and out of bone at a given direction, depending upon the external conditions (physiological plasma [Ca^{2+}] or Ca^{2+} depletion), strongly supports the involvement of bone in the minute-by-minute regulation of plasma calcium but excludes the contribution of bone remodeling in the short term. Of course, calcium depletion in the ECF should be considered as the experimental condition needed to force the calcium efflux from bone and identify its driving force.

On the one hand, the maintenance of the steady calcium influx and its physicochemical nature fits with the following observations: (a) the amount of calcium tracer in bone is increased in hypercalcemic and decreased in hypocalcemic dogs but never reaches saturation level [44]; (b) brushite:apatite mixtures can be equilibrated by cell intervention through secretion of bone matrix proteins giving rise to

[1] Estimation of Ca^{2+} mass transfer rate from/into mice metatarsals to/from ECF. Mouse metatarsus is modeled as a cylinder measuring: 7 mm length, 0.5 mm external diameter, and 0.3 mm medullary cavity diameter (thus, 0.1-mm-thick cortex), closed at both ends by discs of cortical bone of the same thickness. The key parameters to calculate the mass transfer rate per metatarsus have been estimated under the following assumptions: (1) Ca^{2+} exchange takes place primarily at bone quiescent surfaces [9,12]. (2) Total bone surface (T-BS) is the sum of the endo-cortical, intra-cortical, and periosteal surfaces [48]. (3) The sum of endo- and intra-cortical surfaces (eiBS) have been reported to be related to the volume of the cortical bone tissue volume (cTV = 0.88 mm^3) with a ratio such as eiBS/cTV = 3.63 ± 0.75 [48]. Hence, eiBS = 3.19 mm^2. (4) Periosteal surface (Periost-S = 0.99 mm^2) can be approximated to the external 14.18 mm^2. (5) Quiescent bone surfaces (Q-BS) are only a portion of T-BS, and in a cortical growing bone this portion is further reduced since most of the surfaces are either forming or resorbing [12]. Here, Q-BS is estimated between 20% and 50% of T-BS (i.e., Q-BS ranges from 2.84 to 7.09 mm^2). Ca^{2+} mass transfer rate per metatarsus (Φ_m) is calculated multiplying the flux measured at the damage site (~10 pmol cm^{-2} s^{-1}) by the total surface of exchange, i.e., Q-BS. Hence, Φ_m ranges 0.28 to 0.71 pmol s^{-1} $bone^{-1}$, depending on the portion of T-BS taken as Q-BS (20% and 50%, respectively). The corresponding hourly rate ($\Phi_{m/h}$) is: 1.02 to 2.55 nmol/h $bone^{-1}$.

phases capable of buffering calcium over a wide range [45]; (c) whole calvariae from 3-day-old mice were extensively able to buffer increased concentration of calcium in incubation media [46]; (d) hydroxyapatite crystals can determine a net movement of calcium into bone immersed in ECF with supersaturation of calcium and phosphate ions as normally occurs in the secondary mineralization process. This suggests that the influx of calcium into bone is largely passive, thus confirming Neuman and coworker prediction [47]. On the other hand, the maintenance of steady calcium influx at the ECF–BECF interface must have a limited capacity and gradually decline because rapid calcium exchange should be confined to calcium ions at surface positions in the crystal lattice at a maximum depth of 2 μm [48] and the surface-to-volume ratio of the metatarsal bone is rather small. It follows that the influx might not be maintained much longer than the experimental times used unless a return flow to ECF exists (see the pump–leak system section).

The maintenance of the calcium efflux and its cell dependency are in agreement with previous studies [47,49] and appears to be the result of a complex system still undefined. After cell metabolic inhibition, the calcium efflux showed a biphasic pattern characterized by a transient enhancement of the efflux with a subsequent decay, indicating that the available, exchangeable calcium pool might have gone to an equilibrium (no more gradient) which could not be reached in the presence of viable bone cells within the experimental time (~2 h). It follows that an energy-dependent ion exchange system having an ion transporting machinery with specific polarity but not necessarily specific for calcium must exist to maintain the efflux (see the pump–leak system section).

The timeframe to establish (near instantaneous) and the subsequent maintenance of the steady calcium efflux at physiological pH exclude the doubtful [50] osteocytic osteolysis as the source of the efflux as well as the effect of possible acidification of the external medium [51]. The latter was avoided with the addition of 10 mM HEPES that was previously shown [24] to keep pH, pO_2, pCO_2, calculated HCO_3^-, and total CO_2 constant throughout the measurement time [23].

A pump–leak system in the maintenance of calcium fluxes

Even assuming that Ca^{2+} diffuses through the cell interior at the same rate as through water (overestimate), the fluxes measured cannot be transcellular. Although a polarized calcium transport machinery through bone cells has been reported [17–20] and may contribute to the overall calcium translocation, the observed calcium fluxes must occur mainly through paracellular routes along electrochemical and chemical gradients that are generated by a complex multi-ionic pump–leak system, as previously discussed [6,14,23–25,29,52]. By demonstrating that the efflux from bone was dependent on cell viability, while the influx was largely physicochemical, the pump–leak theory of bone involvement in calcium homeostasis gains further confirmation. When the ECF calcium (1.5 mM/L) is higher than BECF calcium (0.5 mM/L), the pump–leak system results in a net calcium influx along the concentration gradient that does not require substantial energy expenditure. Conversely, when the ECF calcium is zero, hence the ECF is at a lower concentration than the BECF (0.5 mM/L), the pump–leak system results in a net calcium efflux from bone along the new outward concentration gradient that requires substantial energy expenditure to be maintained. It is speculated that cells are likely to maintain the steady calcium efflux out of bone at calcium-free ECF through two putative cellular mechanisms: (a) the first assumes a return flow of calcium into the BECF at the intact BECF/ECF interface that closes the calcium loop; this might be driven by either the electrochemical gradient (inside negative) generated by the cells [52] or by the unidirectional and vectorial transcellular calcium transport from the plasma side towards the bone mineral facing side [5,20,53,54]; provided the cells are viable, the loop can be maintained and the flux can be measured; although reliable, this pathway would not play a role in plasma calcium homeostasis; (b) the second assumes that an activated proton secretion, associated in part with H-ATPase, might hydrolyze metastable crystals and generate a continuous loss of calcium from the mineral-facing side [55], thus having a putative fast impact on plasma calcium homeostasis [1]. The amount of calcium released maintains a concentration gradient that is detectable by the SIET at the damage site (point sink) that disappears as the cells die. Although the cellular mechanisms devoted to the maintenance of the efflux can only be hypothesized from the current results, the measurements indicate that the system attempts to fulfill the homeostatic demand, i.e., the very low $[Ca^{2+}]$ in the ECF, by sustaining a steady release of calcium into the ECF without activating remodeling. Without one or all of these mechanisms, the infinite volume of the external medium compared to the finite BECF calcium pool, and the volume-to-surface ratio of the mouse metatarsal bone will rapidly nullify the gradient as was shown here as a result of the inhibition of the bone metabolism.

This view is supported by the calculation of the time necessary to reach equilibrium (T_{eq}) between the BECF and the Ca^{2+}-free ECF by simple diffusion. Calculated T_{eq} fits with the experimental data only if most of the surface available for exchange (Q-BS) is functionally sealed by an active pump–leak system (with the effect of a functional "bone membrane" [14]) as long as the bone is metabolically active. Calcium release from the cell cytosol could only be taken into account to explain the fast calcium efflux transient after poisoning.

Potential location of the bone–plasma interface

The location of the ECF–BECF interface was deduced by the observation of the distribution of calcium gradients in

bone, as follows: (a) presence of a maximal flux at the injury site and over the split cortex (in split bones free of bone marrow), (b) absence of calcium fluxes at the periosteal surface away from the injury site, and (c) presence of a spot flux (in split bones) at the exposed medullary (vascular) facing side. These observations were all consistent with the view that functional compartmentalization of the BECF with respect to the ECF is due to the osteocyte-bone lining cell syncytium [5,14,23–25,29].

Conclusion

Besides the due reasoning in quantitative and qualitative terms, the physiological relevance of the current study relies on the direct real-time measurement of net calcium fluxes which occur at the BECF–ECF interface, following a calcium gradient demand, without the need of hormonal control and/or bone remodeling and which might be implicated in the short-term error correction of plasma calcium. In conclusion, this work extends the longstanding study, started 30 years ago with Bill Neuman, Roy Talmage, Felix Bronner, and Michael Parfitt. As argued by Parfitt [8], ideas regarding how disequilibration levels work between blood and bone might differ, but all agree that an active involvement of bone in plasma calcium homeostasis exists without the need of bone remodeling. The current results are not only consistent with this theory, but make it inescapable. The existence of the functional bone membrane is substantiated and its clinical relevance needs to be explored.

Acknowledgments

Authors are thankful to Dr. Isabella Villa, Bone Metabolic Unit Scient. Inst. H. San Raffael and Prof. Antonio Zaza, Dept. of Biotechnology and Bioscience, University of Milano Bicocca for criticism and advice on the model of calcium fluxes in bone. The support of Prof. Joe Jerry with animal supply and protocols is also greatly appreciated. This study has been sponsored by HSR. The UMass Ion Probe Facility and donations from Applicable Electronics, Inc. to the UMass Biology Dept. Gift Fund made this research possible.

References

[1] Parfitt AM. Bone and plasma calcium homeostasis. Bone 1987;8(Suppl 1):S1–8.
[2] Bronner F, Stein WD. Modulation of bone calcium-binding sites regulates plasma calcium: an hypothesis. Calcif Tissue Int 1992;50:483–9.
[3] Bushinsky DA, Smith SB, Gavrilov KL, Gavrilov LF, Li J, Levi-Setti R. Acute acidosis-induced alteration in bone bicarbonate and phosphate. Am J Physiol: Renal Physiol 2002;283:F1091–7.
[4] Talmage RV, Matthews JL, Mobley HT, Lester GE. Calcium homeostasis and bone surface proteins, a postulated vital process for plasma calcium control. J Musculoskelet Neuron Interact 2003;3:194–200.
[5] Green J, Kleeman CR. Role of bone in regulation of systemic acid–base balance. Kidney Int 1991;39:9–26.
[6] Rubinacci A, Covini M, Bisogni C, Villa I, Galli M, Palumbo C, et al. Bone as an ion exchange system: evidence for a link between mechanotransduction and metabolic needs. Am J Physiol: Endocrinol Metab 2002;282:E851–64.
[7] Bronner F. Extracellular and intracellular regulation of calcium homeostasis. Sci World J 2001;1:919–25.
[8] Parfitt AM. Large calcium fluxes that are not related to remodeling exist. Bone 2003;33:269.
[9] Parfitt AM. Misconceptions (3): calcium leaves bone only by resorption and enters only by formation. Bone 2003;33:259–63.
[10] Heaney RP. How does bone support calcium homeostasis? Bone 2003;33:264–8.
[11] Talmage RV. Perspectives on calcium homeostasis. Bone 2004;35:577–8.
[12] Parfitt AM. Calcium homeostasis. In: Mundy GR, Martin TJ, editors. Handbook of experimental pharmacology, Physiology and Pharmacology of Bone, vol. 107. Heidelberg: Springer-Verlag; 1993. p. 1–65.
[13] Reeve J. The turnover time of calcium in the exchangeable pools of bone in man and the long-term effect of a parathyroid hormone fragment. Clin Endocrinol (Oxford) 1978;8:445–55.
[14] Bushinsky DA, Chabala JM, Levi-Setti R. Ion microprobe analysis of mouse calvariae in vitro: evidence for a “bone membrane”. Am J Physiol 1989;256:E152–8.
[15] Armstrong WD, Singer L. Composition and constitution of the mineral phase of bone. Clin Orthop 1965;38:179–90.
[16] Neuman WF. The milieu interieur of bone: Claude Bernard revisited. Fed Proc 1969;28:1846–50.
[17] Akisaka T, Yamamoto T, Gay CV. Ultracytochemical investigation of calcium-activated adenosine triphosphatase (Ca++-ATPase) in chick tibia. J Bone Miner Res 1988;3:19–25.
[18] Shen V, Hruska K, Avioli LV. Characterization of a (Ca2++ Mg2+)-ATPase system in the osteoblast plasma membrane. Bone 1988;9:325–9.
[19] Stains JP, Gay CV. Asymmetric distribution of functional sodium–calcium exchanger in primary osteoblasts. J Bone Miner Res 1998;13:1862–9.
[20] Stains JP, Weber JA, Gay CV. Expression of Na(+)/Ca(2+) exchanger isoforms (NCX1 and NCX3) and plasma membrane Ca(2+) ATPase during osteoblast differentiation. J Cell Biochem 2002;84:625–35.
[21] Graham CS, Tashjian Jr AH. Mechanisms of activation of Na+/H+ exchange in human osteoblast-like SaOS-2 cells. Biochem J 1992;288(Pt 1):137–43.
[22] Palumbo C, Palazzini S, Marotti G. Morphological study of intercellular junctions during osteocyte differentiation. Bone 1990;11:401–6.
[23] Rubinacci A, De Ponti A, Shipley A, Samaja M, Karplus E, Jaffe LF. Bicarbonate dependence of ion current in damaged bone. Calcif Tissue Int 1996;58:423–8.
[24] Rubinacci A, Benelli FD, Borgo E, Villa I. Bone as an ion exchange system: evidence for a pump–leak mechanism devoted to the maintenance of high bone K(+). Am J Physiol: Endocrinol Metab 2000;278:E15–24.
[25] Borgens RB. Endogenous ionic currents traverse intact and damaged bone. Science 1984;225:478–82.
[26] Bushinsky DA, Goldring JM, Coe FL. Cellular contribution to pH-mediated calcium flux in neonatal mouse calvariae. Am J Physiol 1985;248:F785–9.
[27] Poyart CF, Bursaux E, Freminet A. The bone CO_2 compartment: evidence for a bicarbonate pool. Respir Physiol 1975;25:89–99.
[28] Talmage RV, Lester GE, Hirsch PF. Parathyroid hormone and plasma calcium control: an editorial. J Musculoskelet Neuron Interact 2000;1:121–6.
[29] Rubinacci A, Villa I, Dondi Benelli F, Borgo E, Ferretti M, Palumbo C,

Marotti G. Osteocyte-bone lining cell system at the origin of steady ionic current in damaged amphibian bone. Calcif Tissue Int 1998;63: 331–9.
[30] Scarpace PJ, Neuman WF. The blood: bone disequilibrium: I. The active accumulation of K+ into the bone extracellular fluid. Calcif Tissue Res 1976;137–49.
[31] Bushinsky DA, Levi-Setti R, Coe FL. Ion microprobe determination of bone surface elements: effects of reduced medium pH. Am J Physiol 1986;250:F1090–7.
[32] Kuhtreiber WM, Jaffe LF. Detection of extracellular calcium gradients with a calcium-specific vibrating electrode. J Cell Biol 1990;110: 1565–73.
[33] Smith PJ, Hammar K, Porterfield DM, Sanger RH, Trimarchi JR. Self-referencing, non-invasive, ion selective electrode for single cell detection of trans-plasma membrane calcium flux. Microsc Res Tech 1999;46:398–417.
[34] Pierson ES, Miller DD, Callaham DA, Shipley AM, Rivers BA, Cresti M, et al. Pollen tube growth is coupled to the extracellular calcium ion flux and the intracellular calcium gradient: effect of BAPTA-type buffers and hypertonic media. Plant Cell 1994;6:1815–28.
[35] Franklin-Tong VE, Holdaway-Clarke TL, Straatman KR, Kunkel JG, Hepler PK. Involvement of extracellular calcium influx in the self-incompatibility response of *Papaver rhoeas*. Plant J 2002;29:333–45.
[36] Jaffe LF, Levy S. Calcium gradients measured with a vibrating calcium-selective electrode. Proc IEEE/EMBS Conference 1987;9: 779–81.
[37] Cardenas L, Feijo JA, Kunkel JG, Sanchez F, Holdaway-Clarke T, Hepler PK, et al. Rhizobium nod factors induce increases in intracellular free calcium and extracellular calcium influxes in bean root hairs. Plant J 1999;19:347–52.
[38] Wang R, Pang PK, Wu L, Shipley A, Karpinski E, Harvey S, et al. Neural effects of parathyroid hormone: modulation of the calcium channel current and metabolism of monoamines in identified Helisoma snail neurons. Can J Physiol Pharmacol 1993;71:582–91.
[39] Duthie GG, Shipley A, Smith PJ. Use of a vibrating electrode to measure changes in calcium fluxes across the cell membranes of oxidatively challenged Aplysia nerve cells. Free Radical Res 1994;20: 307–13.
[40] Smith PJ, Sanger RH, Jaffe LF. The vibrating Ca2+ electrode: a new technique for detecting plasma membrane regions of Ca2+ influx and efflux. Methods Cell Biol 1994;40:115–34.
[41] Kunkel JG, Bowdan E. Modeling currents about vitellogenic oocytes of the cockroach, *Blattella germanica*. Biol Bull 1762;89:96–102.
[42] Smit TH, Huyghe JM, Cowin SC. Estimation of the poroelastic parameters of cortical bone. J Biomech 2002;35:829–35.
[43] Bronner F, Aubert JP. Bone metabolism and regulation of the blood calcium level in rats. Am J Physiol 1965;209:887–90.
[44] Brindley GW, Williams EA, Bronk JT, Meadows TH, Montgomery RJ, Smith SR, et al. Parathyroid hormone effects on skeletal exchangeable calcium and bone blood flow. Am J Physiol 1988;255: H94–100.
[45] Neuman WF, Neuman MW, Diamond AG, Menanteau J, Gibbons WS. Blood:bone disequilibrium: VI. Studies of the solubility characteristics of brushite: apatite mixtures and their stabilization by noncollagenous proteins of bone. Calcif Tissue Int 1982;34:149–57.
[46] Messer HH, Yuen SY, Copp DH. Net uptake and release of calcium and phosphate by bone in vitro: effects of medium calcium and phosphate concentrations. Calcif Tissue Res 1975;19:1–7.
[47] Neuman WF, Neuman MW, Myers CR. Blood:bone disequilibrium: III. Linkage between cell energetics and Ca fluxes. Am J Physiol 1979;236:C244–8.
[48] Foldes J, Parfitt AM, Shih MS, Rao DS, Kleerekoper M. Structural and geometric changes in iliac bone: relationship to normal aging and osteoporosis. J Bone Miner Res 1991;6:759–66.
[49] Ramp WK, Demaree DN. Inhibition of net calcium efflux from bone by ethanol in vitro. Am J Physiol 1984;246:C30–6.
[50] Sissons HA, Kelman GJ, Ling L, Marotti G, Cane V, Muglia MA. A light and scanning electron microscopic study of osteocyte activity in calcium-deficient rats. Calcif Tissue Int 1990;46:33–7.
[51] Bushinsky DA, Krieger NS, Geisser DI, Grossman EB, Coe FL. Effects of pH on bone calcium and proton fluxes in vitro. Am J Physiol 1983;245:F204–9.
[52] Trumbore DC, Heideger WJ, Beach KW. Electrical potential difference across bone membrane. Calcif Tissue Int 1980;32:159–68.
[53] Hillsley MV, Frangos JA. Osteoblast hydraulic conductivity is regulated by calcitonin and parathyroid hormone. J Bone Miner Res 1996;11:114–24.
[54] Francis MJ, Lees RL, Trujillo E, Martin-Vasallo P, Heersche JN, Mobasheri A. ATPase pumps in osteoclasts and osteoblasts. Int J Biochem Cell Biol 2002;34:459–76.
[55] George M, Stein B, Muller O, Weis-Klemm M, Pap T, Parak WJ, et al. Metabolic activation stimulates acid secretion and expression of matrix degrading proteases in human osteoblasts. Ann Rheum Dis 2004;63:67–70.